



Angular distribution of the diffuse illuminance

Heliosat-3 project, WP 3030
ENK5-CT-2000-00332

Pierre Ineichen - University of Geneva
Battelle Bâtiment A - 7 rte de Drize
1227 Carouge - Switzerland
February 2005

Abstract

An important input of ray tracing models used in architecture to simulate the luminance distribution in a building is the sky luminance distribution. This parameter is not routinely acquired, even if it is recommended by the CIE. A modelisation of the sky vault luminance distribution based on a radiative transfer models is not feasible with the actual input parameters. A attempt was conducted in Geneva to correlate the asymmetry of a real sky distribution with 41x41 pixels satellite images, but without significant results.

Existing symmetric sky luminance distribution models are evaluated in the present work, and recommendations are given for the use of them.

1. Introduction

Sky luminance distribution for all-weather conditions is the main input for the most recently developed buildings daylighting design tools, and these data are actually not commonly available. Therefore, modelling of this quantity is of high importance to accurately perform daylight estimation in the architectural domain.

Within the Heliosat-3 EC research program, due to the high computer calculation time [Girodo, 2004], a 3D solis RTM approach was not developed. Nevertheless, the luminance angular distribution modelisation is necessary and a correlation between the cloud index and the luminance distribution was studied.

A period of simultaneous acquisition of ground luminance distribution and msg satellite images was used to study the sky luminance distribution.

2. Data

2.1 Sky scanner

The ground measurements are performed with a *EKO Instruments* sky scanner in 145 sky directions, following the CIE recommendations [Tregenza, 1993]. Its measurement head is mounted on a two axis turning table, the luminance sensor is a SI-photodiode with a $V(\lambda)$ filter. An amplifier and an automatic temperature compensation circuit is assembled in the sensor head, the luminance/radiance scan duration for the complete sky vault takes about 3 minutes, the sensor view angle was measured in our laboratory and reaches 11° as represented on Figure 1 [Ineichen 1992, 1993].

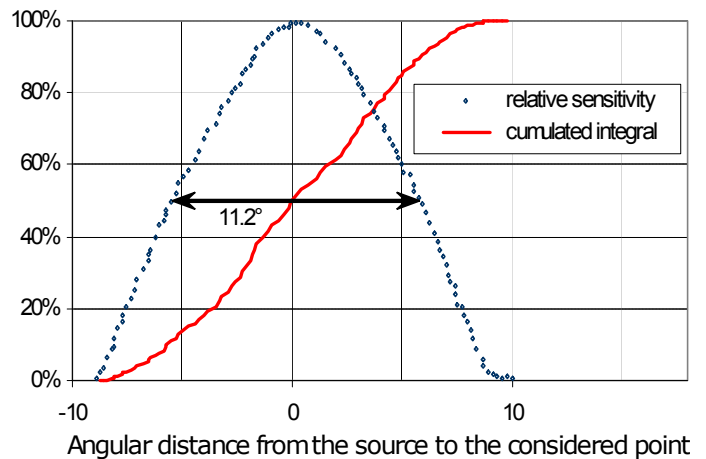


Figure 1 aperture geometry of the Eko sky scanner

In a previous study, an attempt was made to verify the absolute calibration and the stability of the Eko sky scanner by direct comparison with a PRC Krochmann sky scanner, and by comparison of the integrals of the scan with the diffuse illuminance. Due to the bad view geometry of the sensor, and probably electronic instability, a specific calibration of the scanner was not possible, and therefore, the luminance values used in the present study are normalized by the diffuse illuminance.

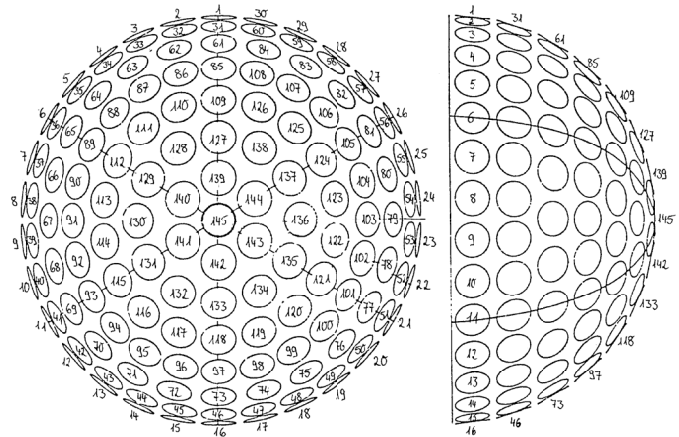


Figure 2 scan geometry of the Eko sky scanner

2.2 Ground measurements

The ground parameters acquisition is synchronized with the satellite images. The EKO instruments sky scanner had multiple time-out problem during the acquisition period and therefore only 10 weeks are available for the present study: from February 7 to February 29, from March 19 to March 30 and from April 5 to May 14. These periods represent a total of 1430 sky scans and 158'000 luminance measurements from 18° above horizon (centre of the solid angle) to the zenith. As a matter of fact, due to the mountains surrounding Geneva and the angle of view of the sky scanner, the measurements centred at 6 degrees above the horizon were never taken into account in the present study.

The corresponding satellite data are 41 pixels x 41 pixels expressed in cloud indices, and centred on the ground station.

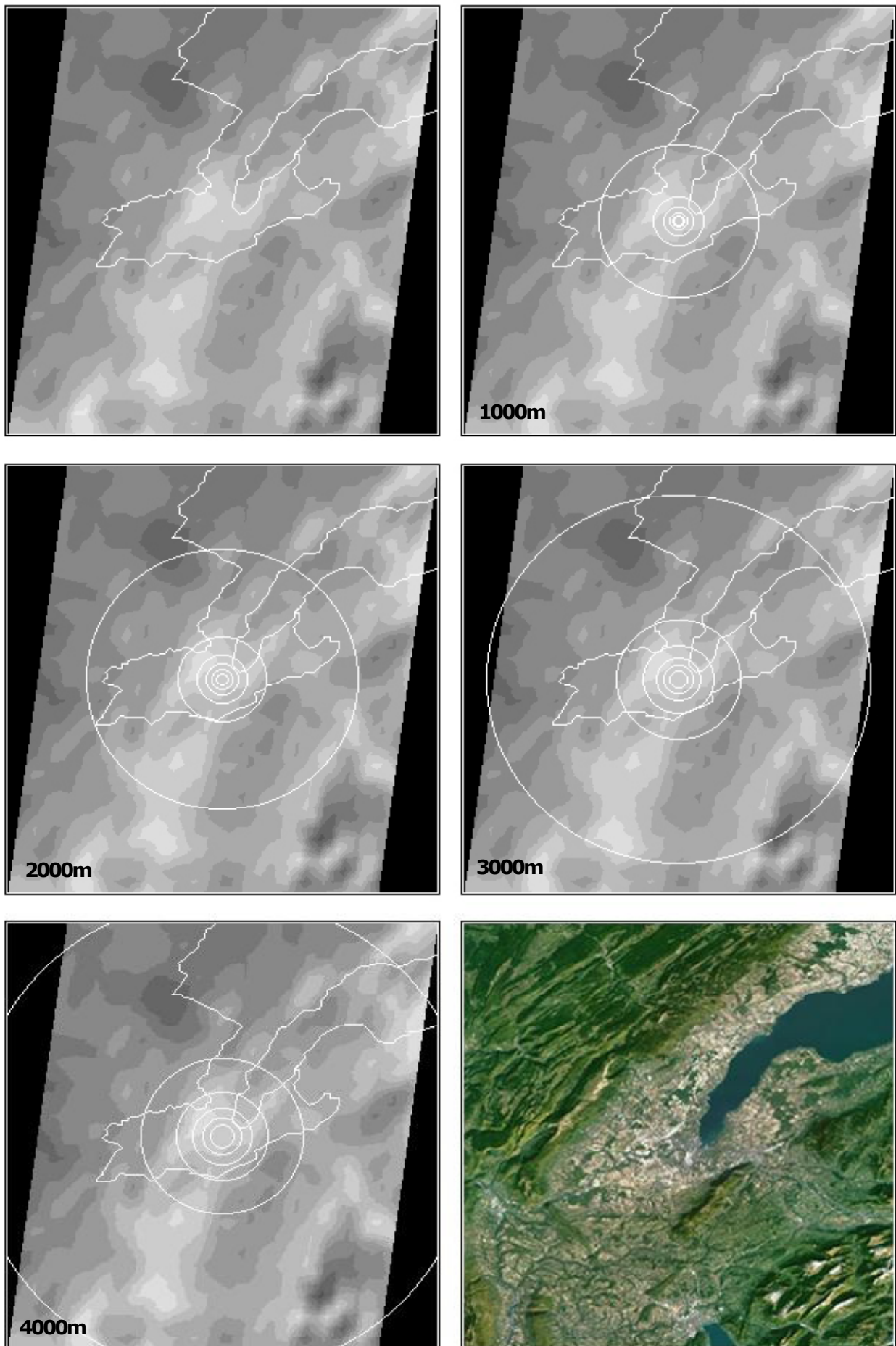


Figure 3 Geometry of the sky vault measurements elevations for different cloud altitudes over the measurement station (1000m, 2000m, 3000m and 4000m)

3. Sky geometry

The satellite view over the Geneva basin can be considered as a limited rectangular plane, extracted from the total disk. It covers the region from Annecy to the Jura. From the sky scanner point of view, the measurement points are equally distributed over the sky dome for fixed 10° of aperture solid angles [Tregenza 1993] as illustrated on Figure 2.

The determination of the pixels seen within each solid angle is dependent of the altitude of the clouds. Figure 3 illustrates the geometry for different altitudes up to 4000 meters above the station. The white circles represent the centre of the solid angle seen by the sensor at a given elevation above the horizon. It can be seen that for clouds at 3000 meters, the measurements at 18° above the horizon cover the complete extracted region.

4. Satellite-ground comparison

Comparing the extracted field from the satellite image and the ground sky scans raised some difficulties. The first problem comes from the cloud availability. In particular cases, like for Geneva, it is possible to obtain from the Swiss Meteorological Institute the cloud altitude on a 3 hours basis, but in the view of an automatic routine luminance production, it is not an evidence. The second problem is due to the geometry: the sky scanner sees the sky vault from the ground (the lowest part of the clouds) and the satellite from the space, that is the top of the clouds. It is therefore difficult to combine a given region seen by the satellite with the corresponding region seen by the scanner.

In order to overcome these problems, a constant average cloud altitude was used (2500m) to spatially synchronise the two sets of data. The second step was to integrate the luminance and the cloud index over the same sky regions. The sky scanner data integration is easy to do and, if done over the complete sky vault (except the sun position region), gives the diffuse illumination. The same method was used for the cloud indices. Considering a constant cloud altitude, each pixel has a fixed elevation over the horizon and the weighting factor will be trigonometric. The cloud index integral is then normalized to its maximum value. For both of the integration, a 15 degrees angular distance from the sun region is removed from the calculation.

Dividing the sky vault in the four cardinal regions and comparing the cloud index integrals with the luminance integrals gives a very high dispersion and no correlation could be pointed out. This is probably due to the ambiguity between the blue sky and the dark cloud in term of luminance. In fact, a clear sky region will conduct to a low luminance value and a low cloud index, while a high overcast sky region will show a low luminance value and a high cloud index. This is illustrated on Figure 4 where it can be seen that for the same

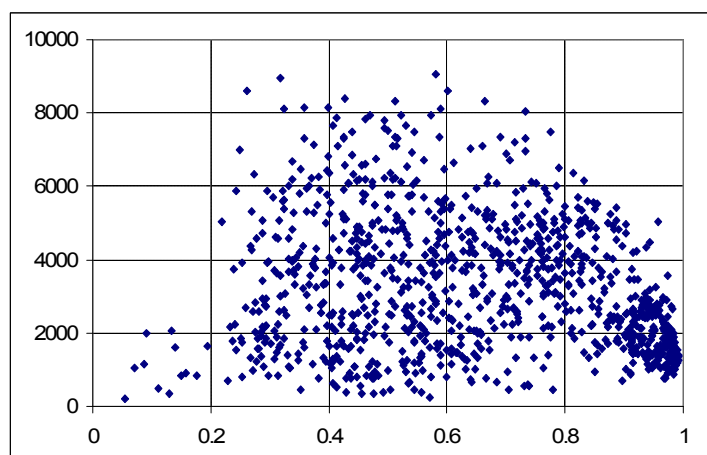


Figure 4 Integrated luminance versus integrated cloud index (see text)

luminance integral, the normalized integrated cloud index can vary from 0.2 to 1.

The distinction between the two occurrences could probably be improved with a cloud mask and the knowledge of the top and bottom cloud altitude, but even with these supplemental inputs, the short period of measurements considered in this study is certainly not sufficient to do a robust analyze of the parameter dependence.

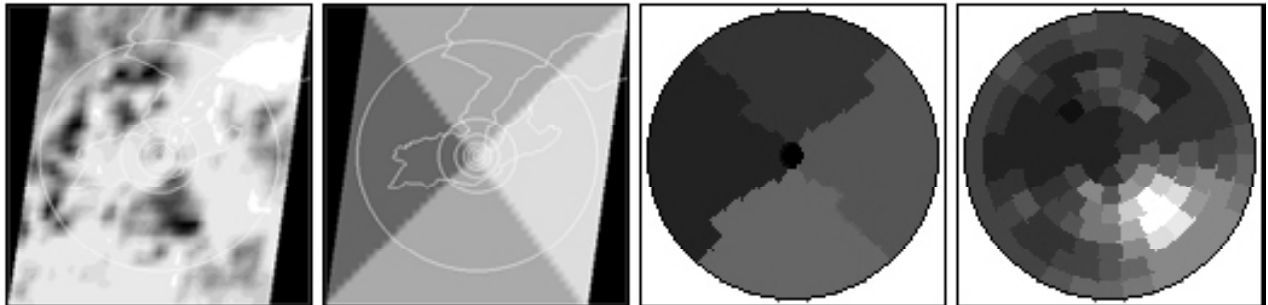


Figure 5 Left: cloud index normalized integral and right the corresponding integrated luminance in the four cardinal directions.

As a lot of luminance distribution models exist in the literature based on irradiance/illuminance inputs and for some of them based on RTM calculations, it is wiser to concentrate in producing high quality inputs to well assessed existing indirect models.

5. Luminance distribution models

5.1 Brunger model

The model is a three-component continuous model and was originally developed for modelling the sky radiance; it is a superposition of three terms, isotropic, circumsolar, and horizontal brightening factor. The weighting parameters are D_h/G_h and the clearness index K_t [Brunger 1985].

5.2 Matsuzawa model

This model is a combination of the three CIE standard skies: clear, intermediate, and overcast [CIE 1973]. The governing parameter is an illuminance «cloud ratio» defined as D_{vh}/G_{vh} [Matsuura 1990].

5.3 ASRC-CIE model

Perez et al. [Perez 1992] modified Matsuzawa's model to take into account the high turbid intermediate skies. The interpolating parameters are Perez' epsilon and delta (clearness and brightness respectively) coefficients. We reference here two versions of the model [Perez 1990, 1992]; the best results are obtained with the most recent version, which was used in this study.

5.4 Perez model

Five coefficients describe the quality and the quantity of the luminance of the sky dome. Each of the coefficients has a specific physical effect and depends on the sky clearness and sky brightness: (a) darkening or brightening of the horizon region; (b) luminance gradient near the horizon; (c) relative intensity of the circumsolar region; (d) width of the circumsolar region; and (e) the relative backscattered light [Perez 1993].

5.5 Perraudau model

The formulation of the model is a product of three functions, depending respectively on the angular distance to the sun (zeta), the height of the considered point, and the sun elevation. The five discrete sky conditions are parameterized with a nebulosity index, which is a normalized cloud ratio [Perraudau 1990] .

5.6 Harrison model

The Harrison model needs an opaque cloud cover to combine two basic luminance distributions: clear and cloudy sky. We used a normalized D_h/G_h coefficient as opaque cloud cover [Harrison 1993].

5.7 Kittler model

Based on the light diffusion theory, the Kittler model is a complex formula that calculates the absolute or relative sky luminance pattern. The governing parameter is the atmospheric illuminance turbidity [Kittler 1986].

5.8 Igawa model

This model is the most recently published model. The governing parameters are retrieved from the horizontal irradiance values; they are the clear sky index and a cloud ratio index. The model is a weighting of the CIE standard clear sky and the CIE standard overcast sky [Igawa 2004].

5.9 Gueymard model

This empirical clear sky model was developed in 1986 [Gueymard 1986] and is based on measurements made in Berkeley. The luminance distribution is obtained by combination of a hemispherical component (weakly turbidity dependent) and a circumsolar component (highly turbidity dependent). An average turbidity is used over the considered periods and a cloud opacity (calculated on the basis of the diffuse fraction) is used as weighting coefficient between the clear sky and a completely overcast sky.

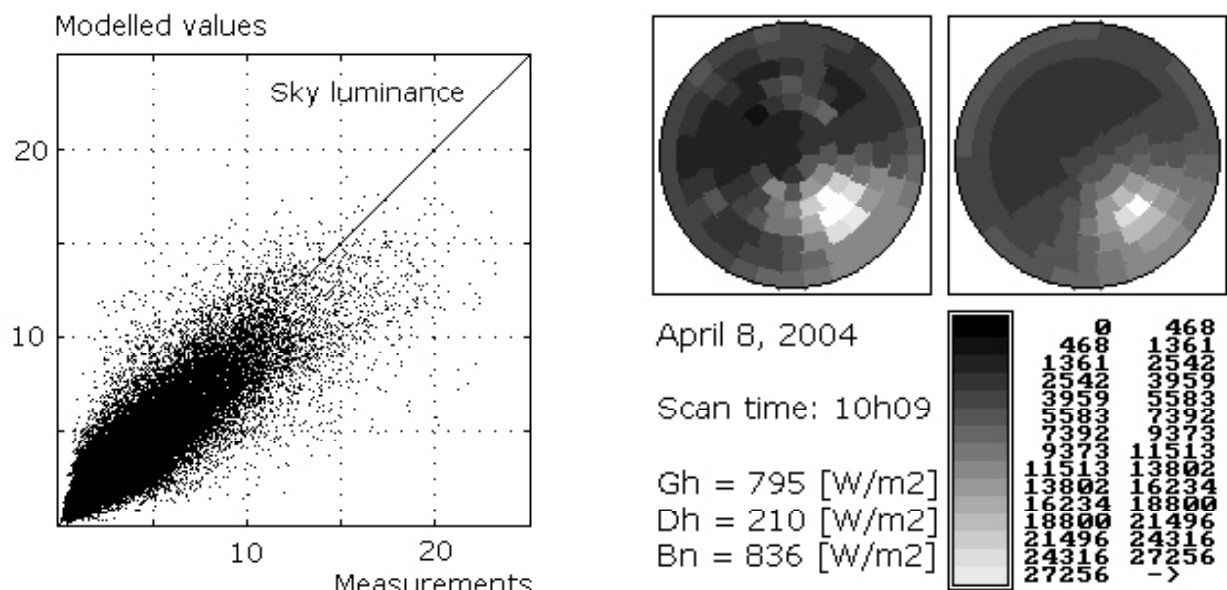


Figure 6 Illustration of the Perez model. Left: modelled luminance versus measurements for all the considered data. Right: measured and modelled scan for April 8, 2004

5.10 Isotropy hypothesis

The inclusion of an isotropic luminance distribution in the sky vault is made to have a reference behaviour. This hypothesis is not realistic, even for completely overcast conditions (i.e. CIE overcast sky [CIE 1973]).

6. Model validation

For the 1430 sky scans (i.e. the 158'000 luminance measurements) a root mean square difference (rmsd) is calculated. Considering that the models give either relative or absolute luminance values, and that the sky scanner was not specifically calibrated in our centre (see section 2), the evaluated luminance distributions were normalized to the integral of the measured luminance (this represents the horizontal diffuse illuminance without the horizon band from 0° to ~12°). In this case, the bias will always be zero and the comparison parameter will come down to the rmsd. Table I illustrates the comparison.

Model	rmsd [cd/m ²]	
ASRC-CIE	1931	36%
Brunger	2092	39%
Gueymard	3169	60%
Harrison	2127	40%
Igawa	1969	37%
Isotrope	3477	65%
Kittler	2418	45%
Matzuzawa	2159	41%
Perez	1899	36%
Perraudeau	2188	41%
Average luminance	5323	

Table I rmsd of the luminance models in alphabetical order

From the table, it can be seen that the ASRC-CIE and the Perez models give the best results. The ASRC-CIE model is a combination of four specific sky conditions, while the Perez model (Figure 6) is mathematically continuous, slightly better but also slightly more computer-time consuming.

As absolute luminances are not available with the Eko scanner used in this study, the comparison was conducted on normalized values. The use of satellite derived input data will therefore not have a significant influence on the above rmsd (maximum of 2% increase). As a matter of fact, due to the normalization, the root mean square difference is inherent to the luminance distribution models, and a slight increase of the rmsd will appear if the model needs booth global and direct/diffuse irradiances as input.

8. Conclusion

In the present context and taking into account the small quantity of data and input parameters, it was not possible to increase the accuracy of the sky luminance distribution models.

A performance comparison was conducted on a 10 weeks measurements period for 9 models that confirm previously published validations. Two models are slightly better, the ASRC-CIE and the Perez Model. The first is a discreet model based on look-up tables, the second is a mathematically continuous model.

All the models use irradiance or illuminance components as input parameters. The conclusion of the present study is that the indirect way (i.e. evaluation of the sky luminance distribution on the basis of irradiance and/or illuminance parameters) still gives the best results, even if the sky distribution can only be symmetrically modelled. The modelled luminances are normalized by the diffuse illuminance; it is therefore important to have access to good quality input parameters.

9. Bibliography

Brunger, A. P., and Hooper, F. C., Anisotropic sky radiance model based on narrow field of view measurements of shortwave radiance, *Solar Energy* 51(1), 53-64 (1993).

CIE. Standardization of luminance distribution on clear skies. CIE publication N° 22 (TC-4.2), (1973)

Gueymard Ch.. Une paramétrisation de la luminance énergétique du ciel clair en fonction de la turbidité. *Atmos. Ocean* 24 (1), pp 1-15, (1986)

Harrison, A. W., Directional sky luminance versus cloud cover and solar position, *Solar Energy* 46(1), 13-19 (1991).

Igawa N., Koga Y., Matsuzawa T., Nakamura H. Models of sky radiance distribution and sky luminance distribution *Solar Energy* 77,137-157, (2004)

Ineichen, P., Molineaux, B., PRC sky scanner characterisation, cosine dependence, aperture angle of NPB, CUEPE, University of Geneva, (1992).

Ineichen, P., and Molineaux, B., Characterisation and comparison of two sky scanners: PRC Krochmann and EKO Instruments, Internal report, Groupe of Applied Physics, University of Geneva, Switzerland (1993).

Kittler, R., Luminance model of homogeneous skies for design and energy performance predictions, 2nd International Daylighting Conférence, Long Beach, CA (1986).

Matsuura, K., and Iwata, T., A model of daylight source for the daylight illuminance calculations on all weather conditions, CIE Daylighting Conference, Moscow (1990).

Switzerland (1993).

Perez, R., Ineichen, P., Seals, R., Michalsky, J., and Stewart, R., Modelling daylight availability and irradiance components from direct and global irradiance, *Solar Energy* 44(5), 271-289 (1990).

Perez, R., Michalsky, J., and Seals, R., Modelling sky luminance angular distribution for real sky conditions. Experimental evaluation of existing algorithms, J. Illumin. Engg. Soc. 21(2), 84-92 (1992).

Perez, R., Seals, R., and Michalsky, J., An all-weather model for sky luminance distribution, Solar Energy, 50(3), 235-245 (1993).

Perraudeau, M., Daylight availability from energetic data, CIE Daylighting Conference, Moscow, Vol. I, pp. A17 (1990).

Tregenza, P. R., Perez, R., Michalsky, J., and Seals, R., Guide to recommended practice of daylight measurement, CIE TC-3.07, (1993).